Pure Appl. Chem., Vol. 77, No. 10, pp. 1707–1717, 2005.
DOI: 10.1351/pac200577101707

Synthesis and single-crystal structure analysis of a new layered zinc phosphate*

Natasa Zabukovec Logar[1], Nevenka Rajic[1,2], Djordje Stojakovic[2], Amalija Golobic[3], and Venceslav Kaucic[1,4,‡]

[1]National Institute of Chemistry, Hajdrihova 19, 1000 Ljubljana, Slovenia; [2]Faculty of Chemical Technology and Metallurgy, University of Belgrade, Karnegijeva 4,11000 Belgrade, Serbia; [3]Faculty of Chemistry and Chemical Technology, University of Ljubljana, Askerceva 5, 1000 Ljubljana, Slovenia; [4]Biotechnical Faculty, University of Ljubljana, Jamnikarjeva 101, 1000 Ljubljana, Slovenia

Abstract: A new 2D zinc phosphate $[H_3NCH(CH_3)CH_2NH_3]^{2+}{}_{0.75}[COOH(CH_2)COOH]_{0.25}(Zn_3P_3O_{11}OH)^{2-}{}_* 0.5NH_4^+$ consists of zinc phosphate layers, which are intercalated by diprotonated 1,2-diaminopropane, malonic acid, and NH_4^+ ions. The inorganic layers are composed of alternating ZnO_4 and PO_4 (PO_3OH) tetrahedra that form 8-membered ring apertures. The intercalated species strongly interact with the zinc phosphate layers through hydrogen bonds, which is a key factor in stabilizing the structure. Crystal data: monoclinic, $P2_1/a$, a = 8.3457(1) Å, b = 16.8953(3) Å, c = 10.1817(2) Å, β = 95.3121(8)°, Z = 4, R = 0.0423.

Keywords: Layered; zinc phosphate; open framework; low-dimensional; ZPAM.

INTRODUCTION

In the last decade, many open-framework zinc phosphates have been synthesized. Among them there are the 3D architectures [1–14] but also the low-dimensional ones, 2D layers [15–21] as well as 1D chains [22,23]. Recently, even 0D four-membered ring monomers have been reported [24,25]. Structural diversity of the zinc phosphates has still been expanded by the possibility of the low-dimensional structures to transform to complex ones under ordinary reaction conditions [25,26].

Recently, it has been found that some of organic ions can be used as a building block to construct novel hybrid inorganic–organic open frameworks. Thus, open-framework zinc oxalate–phosphates have also been reported [27–29]. In the reported structures, oxalate ions possess a bridging role holding together the zinc phosphate layers. It seems likely that the introduction of such building blocks gives rise to the possibility of tuning the space between the layers (i.e., pore dimensions) by a selection of the appropriate organic species.

This gives us an idea to investigate other dicarboxylate ligands as possible pillars in the construction of novel zinc phosphate structures. Thus, malonate complexes show an enhanced structural diversity owing to the versatility of this ligand, which can adopt different coordination modes [30]. Also, it has recently been found that malonate ions have the ability to be structurally involved in a 3D lattice formation [31]. Here, we report the structure of a zinc phosphate (ZPAM) obtained using malonic acid (H_2mal) and 1,2-diaminopropane (DAP).

---

*Paper based on a presentation at the 4th International Conference of the Chemical Societies of the South-Eastern European Countries (ICOSECS-4), Belgrade, Serbia and Montenegro, 18–21 July 2004. Other presentations are published in this issue, pp. 1655–1752.

‡Corresponding author

EXPERIMENTAL

The ZPAM was synthesized hydrothermally under autogenous pressure using zinc acetate dihydrate ($Zn(ac)_2$, Aldrich), orthophosphoric acid (H_3PO_4, 85 wt %, Fluka), DAP (99 wt %, Aldrich), H_2mal (Aldrich), H_2O, and ethylene glycol (Merck) in the molar ratios of 1:6:1:2:100:100. A typical synthesis involves the dissolving of 10 mmol $Zn(ac)_2$, 60 mmol H_3PO_4, and 20 mmol DAP in 10 cm^3 H_2O. The solution of 10 mmol H_2mal in 9 cm^3 ethylene glycol was added dropwise in the last step to the aqueous solution of other reagents. The resulting solution was transferred into a 50-ml Teflon-lined stainless steel autoclave, which is then heated at 135 °C for 10 days. The initial pH was about 2.5, and it slightly decreased to 2 by the end of reaction. The obtained white product (ZPAM) is filtered off and washed with demineralized water.

Zinc and phosphorous were analyzed by the inductively coupled plasma emission spectroscopy, while carbon, hydrogen, and nitrogen were determined with a standard C,H,N analyzer. The crystal morphology was analyzed using a JEOL 5800 SEM. Thermogravimetric analyses and differential scanning calorimetry (TGA and DSC) were performed using a SDT 2960 Simultaneous DSC-TGA instrument (TA Instruments) at a heating rate of 10 °C/min under a helium flow.

A colorless needle-like single crystal ($0.35 \times 0.015 \times 0.012$ mm^3) of ZPAM was selected for the X-ray structure analysis. The low-temperature intensity data were collected on a Nonius Kappa CCD diffractometer by using the MoK_α radiation to eliminate possible dynamic disorder in the structure. Unit cell parameters were determined by least-square refinement on the basis of 3380 reflections. The structure was solved combining the SIR97 [32] and Fourier map calculation using the SHELXL-97 [33]. The latter program was also used for the structure refinement and the interpretation. The intercalated organic cations and molecule were refined with partial occupancies, with a following scheme: two positions of H_2DAP^{2+} cation with partial occupancies of 50 and 25 %, one position of malonic acid 25 % occupied, and one position of amine cation 50 % occupied. Both cations and molecule were refined with restraints on bond distances. The hydrogen atoms were located in a different Fourier map (attached to the inorganic layer) or were included at calculated positions (attached to the organic molecule and cations). All non-hydrogen atoms from the inorganic layers were anisotropically refined and those from overlapping organic species isotropically. Final atomic parameters with bond distances are presented in Tables 2–4. A brief summary of the crystallographic data is given in Table 1. Crystallographic data (excluding structure factors) for the structure reported in this paper have been deposited with the Cambridge Crystallographic Data Centre as supplementary publication no. CCDC 251046. Copies of the data can be obtained free of charge on application to CCDC, 12 Union Road, Cambridge CB2 1EZ, UK (Fax: (44) 1223 336-033; E-mail: deposit@ccdc.cam.ac.uk).

Table 1 Experimental conditions and crystallographic data for the single X-ray diffraction study.

Formula of asymmetric unit	C3 H13 N2 O13 P3 Zn3
Formula weight	574.17
Crystal system	monoclinic
a (Å)	8.34570(1)
b (Å)	16.8953(3)
c (Å)	10.1817(2)
β (°)	95.3121(8)
V (Å^3)	1429.49(4)
Space group	$P2_1/a$
D_c (g·cm^{-3})	2.667
Crystal size (mm^3)	0.35 × 0.015 × 0.012
T (K)	150(2)
$\lambda(MoK_\alpha)$ (Å)	0.71073
hkl-data limits	$-10 \le h \le 10$, $-21 \le k \le 21$, $-13 \le l \le 13$
θ_{max} (°)	27.53
R_{merge}	0.0216
μ (MoK_α) (mm^{-1})	5.405
Total data	6312
Observed data [$F^2 \ge 2\sigma(F^2)$]	2735
Refined data	3282
Parameters	205
R (on F^2)	0.0423
R_w (on F^2)	0.1311
$\Delta\rho_{max}$ (e Å^{-3})	1.181
$\Delta\rho_{min}$ (e Å^{-3})	–1.112

Table 2 Fractional atomic coordinates and equivalent displacement parameters (Å^2). The two positions of the atoms from disordered 1,2-diamine cation are labeled with extension *a* (50 % occ.) or *b* (25 % occ.) and atoms from malonate molecule with extension *c* (25 % occ.).

	Ueq = (1/3) $\Sigma_i\Sigma_j U_{ij}a_i^*a_j^*a_ia_j$.				
	x	y	z	Ueq	Part. occ.
P1	0.57723(17)	0.37646(8)	0.91707(13)	0.0150(3)	
P2	1.17502(16)	0.33814(8)	1.19023(13)	0.0148(3)	
P3	0.63874(17)	0.37472(8)	1.45265(13)	0.0155(3)	
Zn1	1.41303(8)	0.23349(4)	1.35713(6)	0.0169(2)	
Zn2	0.87019(8)	0.26811(4)	1.01582(6)	0.0159(2)	
Zn3	0.48354(7)	0.45121(4)	1.18408(6)	0.0158(2)	
O1	1.2981(5)	0.2681(2)	1.1885(4)	0.0198(8)	
O2	1.0585(5)	0.3322(3)	1.0678(4)	0.0246(9)	
O3	1.0921(5)	0.3324(3)	1.3172(4)	0.0222(9)	
O4	1.2643(5)	0.4166(2)	1.1890(4)	0.0210(8)	
O5	0.6110(5)	0.4274(3)	1.0418(4)	0.0280(10)	
O6	0.6397(5)	0.4244(3)	1.3289(4)	0.0279(10)	
O7	0.5430(5)	0.4327(2)	0.7971(4)	0.0167(8)	
O8	0.7870(5)	0.3226(3)	1.4734(4)	0.0241(9)	
O9	0.6487(5)	0.4381(3)	1.5674(4)	0.0250(9)	
H9	0.5635	0.4387	1.6016	0.0460(18)	

(*continues on next page*)

Table 2 (*Continued*).

	Ueq = (1/3) $\Sigma_i\Sigma_j U_{ij} a_i^* a_j^* a_i a_j$.				
	x	y	z	Ueq	Part. occ.
O10	0.4837(5)	0.3273(3)	1.4590(4)	0.0251(9)	
O11	0.7255(5)	0.3272(3)	0.8959(4)	0.0256(9)	
O12	0.4264(5)	0.3261(3)	0.9242(4)	0.0294(10)	
C3a	0.869(2)	0.6873(10)	1.304(2)	0.0460(18)	0.5
H31a	0.7616	0.7059	1.3102	0.0460(18)	0.5
H32a	0.8961	0.6926	1.2148	0.0460(18)	0.5
H33a	0.9429	0.7180	1.3614	0.0460(18)	0.5
C2a	0.881(2)	0.6018(10)	1.3442(19)	0.0460(18)	0.5
H2a	0.9387	0.6165	1.4288	0.0460(18)	0.5
N2a	0.7377(17)	0.5904(9)	1.4066(15)	0.0460(18)	0.5
H21a	0.6717	0.6311	1.3886	0.0460(18)	0.5
H22a	0.7617	0.5869	1.4934	0.0460(18)	0.5
H23a	0.6899	0.5459	1.3770	0.0460(18)	0.5
C1a	0.980(2)	0.5392(10)	1.3335(16)	0.0460(18)	0.5
H11a	0.9179	0.4907	1.3265	0.0460(18)	0.5
H12a	1.0550	0.5357	1.4123	0.0460(18)	0.5
N1A	1.0672(17)	0.5470(9)	1.2222(13)	0.0460(18)	0.5
H13a	1.1471	0.5120	1.2269	0.0460(18)	0.5
H14a	1.1074	0.5957	1.2197	0.0460(18)	0.5
H15a	1.0018	0.5383	1.1495	0.0460(18)	0.5
C3b	0.913(2)	0.6808(11)	1.302(2)	0.0050(15)	0.25
H31b	0.8669	0.7216	1.3528	0.0050(15)	0.25
H32b	0.9009	0.6948	1.2106	0.0050(15)	0.25
H33b	1.0251	0.6752	1.3313	0.0050(15)	0.25
C2b	0.822(2)	0.5983(10)	1.3231(16)	0.0050(15)	0.25
H2b	0.7228	0.6015	1.2634	0.0050(15)	0.25
N2b	0.7640(19)	0.5890(10)	1.4589(15)	0.0050(15)	0.25
H21b	0.7418	0.5383	1.4728	0.0050(15)	0.25
H22b	0.6758	0.6180	1.4642	0.0050(15)	0.25
H23b	0.8406	0.6053	1.5195	0.0050(15)	0.25
C1b	0.935(2)	0.5385(10)	1.2513(16)	0.0050(15)	0.25
H11b	1.0466	0.5558	1.2549	0.0050(15)	0.25
H13b	0.9292	0.4843	1.2820	0.0050(15)	0.25
N1b	0.8467(19)	0.5518(9)	1.1245(14)	0.0050(15)	0.25
H13b	0.8821	0.5189	1.0653	0.0050(15)	0.25
H14b	0.8608	0.6015	1.0994	0.0050(15)	0.25
H15b	0.7425	0.5431	1.1308	0.0050(15)	0.25
O14c	0.744(6)	0.673(3)	1.348(6)	0.193(13)	0.25
H14c	0.6870	0.6340	1.3556	0.193(13)	0.25
O15c	0.983(7)	0.684(4)	1.258(7)	0.193(13)	0.25
C3c	0.897(7)	0.650(3)	1.327(7)	0.193(13)	0.25
C2c	0.882(10)	0.563(3)	1.296(6)	0.193(13)	0.25
H21c	0.7811	0.5523	1.3322	0.193(13)	0.25
H21c	0.9628	0.5428	1.3624	0.193(13)	0.25
C1c	0.881(7)	0.493(3)	1.198(6)	0.193(13)	0.25
O16c	1.027(7)	0.453(3)	1.240(6)	0.193(13)	0.25

(*continues on next page*)

Table 2 (*Continued*).

Ueq = (1/3) $\Sigma_i\Sigma_j U_{ij} a_i^* a_j^* a_i a_j$.					
	x	y	z	Ueq	Part. occ.
H16c	1.0891	0.4570	1.1829	0.193(13)	0.25
O17c	0.887(9)	0.527(4)	1.090(5)	0.193(13)	0.25
N3	0.8901(16)	0.4962(8)	1.0137(13)	0.038(3)	0.5
H31	0.965(11)	0.474(7)	0.971(10)	0.0460(18)	0.5
H32	0.829(12)	0.460(5)	1.042(11)	0.0460(18)	0.5
H33	0.936(14)	0.521(6)	1.083(7)	0.0460(18)	0.5
H34	0.837(12)	0.529(5)	0.961(9)	0.0460(18)	0.5

Table 3 Selected bond distances (Å).

P1-O11	1.523(5)	Zn1-O8	1.907(4)
P1-O12	1.527(5)	Zn1-O3	1.936(4)
P1-O5	1.539(4)	Zn1-O10	1.956(4)
P1-O7	1.553(4)	Zn1-O1	1.976(4)
P2-O2	1.511(4)	Zn2-O11	1.916(4)
P2-O4	1.521(4)	Zn2-O12	1.924(5)
P2-O3	1.525(4)	Zn2-O2	1.942(4)
P2-O1	1.568(4)	Zn2-O1	2.006(4)
P3-O6	1.514(4)	Zn3-O5	1.918(4)
P3-O8	1.518(4)	Zn3-O4	1.926(4)
P3-O10	1.528(5)	Zn3-O6	1.930(4)
P3-O9	1.582(5)	Zn3-O7	1.984(4)
C3a-C2a	1.50(2)	C1b-N1b	1.45(2)
C2a-C1a	1.36(2)		
C2a-N2a	1.42(2)	O14c-C3c	1.37(3)
C1a-N1a	1.41(2)	O15c-C3c	1.20(3)
		C3c-C2c	1.51(3)
C3b-C2b	1.61(2)	C2c-C1c	1.53(3)
C2b-N2b	1.51(2)	C1c-O17c	1.25(3)
C2b-C1b	1.61(2)	C1c-O16c	1.43(3)

Table 4 Selected H-bond distances (Å).

N1a-O4	2.79(1)		
N1a-O11	3.06(1)	O14c-O10	2.85(5)
N1a-O9	3.06(1)	O14c-O15c	2.29(8)
N2a-O6	3.01(2)	O16c-O3	2.24(6)
N2a-O7	3.01(2)	O17c-O4	2.19(6)
N2a-O10	2.77(2)		
		N3-N1a	2.57(2)
N1b-O2	2.93(1)	N3-O2	3.06(9)
N1b-O5	2.95(2)	N3-O4	2.76(1)
N2b-O3	2.81(2)	N3-O5	2.64(1)
N2b-O9	2.97(2)		
N2b-O10	2.70(2)	O9-O7	2.576(6)

RESULTS AND DISCUSSION

SEM analysis revealed a needle-like morphology of the as-synthesized ZPAM as illustrated in Fig. 1. Thermal analysis shows an overall weight loss of about 17 wt % (Fig. 2), which is in agreement with the C,H,N analysis. The first loss of about 1 % is accompanied by a broad maximum in the dtg curve centered at 120 °C, corresponding to the physically adsorbed water molecules. The second (major) weight loss (~15 %) proceeds in several steps (with the maxima in the dtg curve at 355, 385, and 467 °C), corresponding to decomposition of intercalated species (calc. 15.5 %). Elemental analysis performed by the inductively coupled plasma emission spectroscopy gave an overall chemical formula of ZPAM as follows:

$$[H_3NCH(CH_3)CH_2NH_3]^{2+}{}_{0.75}[COOH(CH_2)COOH]_{0.25}(Zn_3P_3O_{11}OH)^{2-}{}_{*}0.5NH_4{}^{+}$$

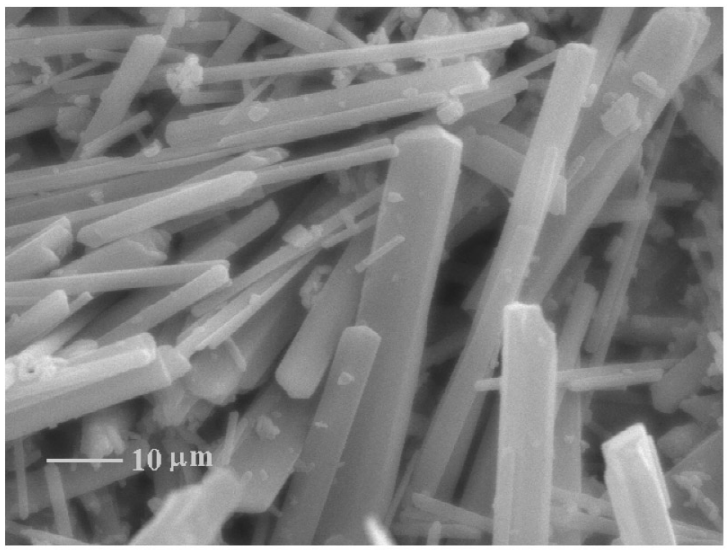

Fig. 1 SEM picture of ZPAM.

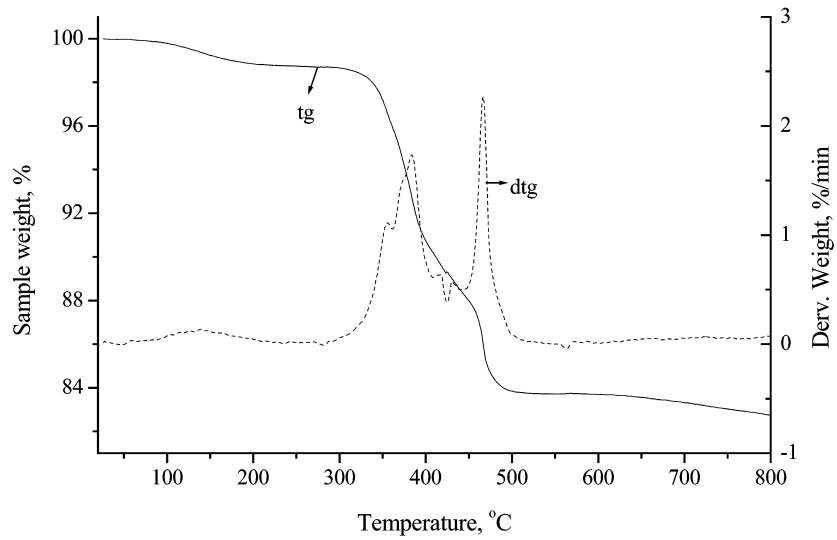

Fig. 2 Tg/dtg curves of ZPAM.

Single-crystal X-ray structure analysis showed that ZPAM crystallizes in a monoclinic space group $P2_1/a$ with lattice parameters, a = 8.3457(1) Å, b = 16.8953(3) Å, c = 10.1817(2) Å, β = 95.3121(8)°. The crystal structure is built up of corrugated macroanionic zinc phosphate layers $[Zn_3P_3O_{11}OH]^{2-}$ that propagate in the [100] plane and possess 8-membered ring apertures (Fig. 3). Between these layers lay interspersed NH_4^+ ions, H_2DAP^{2+} ions, and malonic acid molecules; the former two cations also serve to compensate for negatively charged layers. The packing of zinc phosphate layers and intercalated organic species is shown in Fig. 4.

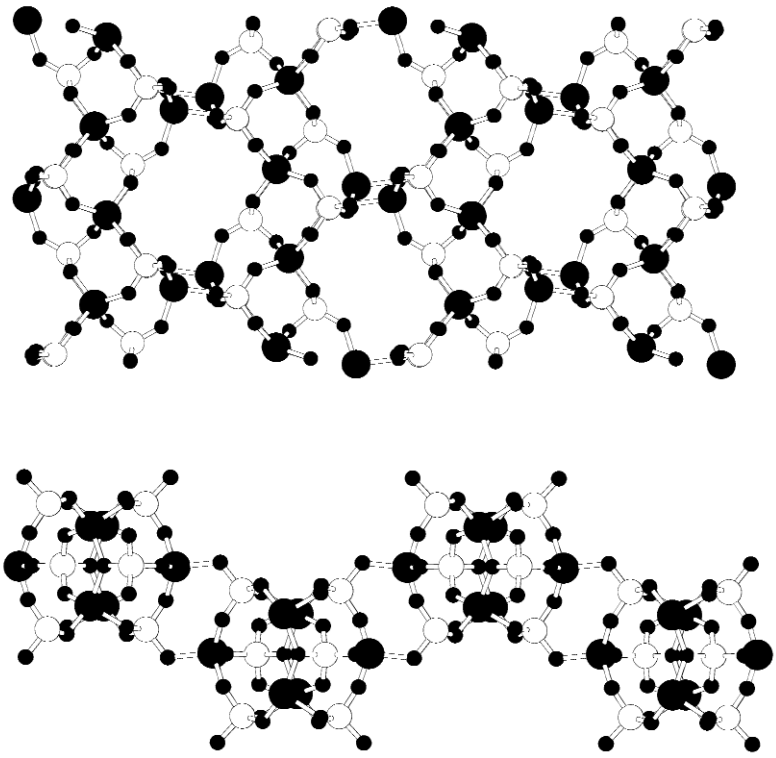

Fig. 3 Schematic presentation of zinc phosphate layers along z-axis (top) and x-axis (bottom); Zn = big solid circles, P = open circles, O = small solid circles.

There are three crystallographically distinct zinc sites and three phosphorous sites in the asymmetric unit (Fig. 4). All Zn atoms are tetrahedrally coordinated and share four oxygen atoms with the adjacent P atoms. The Zn–O bond lengths are in the range from 1.907(4) to 2.006(4) Å (Table 3) and the O–Zn–O bond angles from 98.4(2)° to 123.4(2)°. The P–O bond lengths in PO_4 and $PO_3(OH)$ tetrahedra range from 1.511(4) to 1.582(5) Å, as shown in Table 3, and are comparable with values in similar structures [34]. The longest P–O bond of 1.584(4) Å [P(3)–O(9)] indicates the presence of a P–OH connection. The O–P–O bond angles range from 103.6(3)° to 113.3(2)°. An interesting feature is a trigonal coordination of one of the 12 oxygen atoms in the inorganic layer, O(1), which is bonded to two zinc and one phosphorous atom with bond lengths of 1.976(4), 2.006(4), and 1.568(4) Å, respectively.

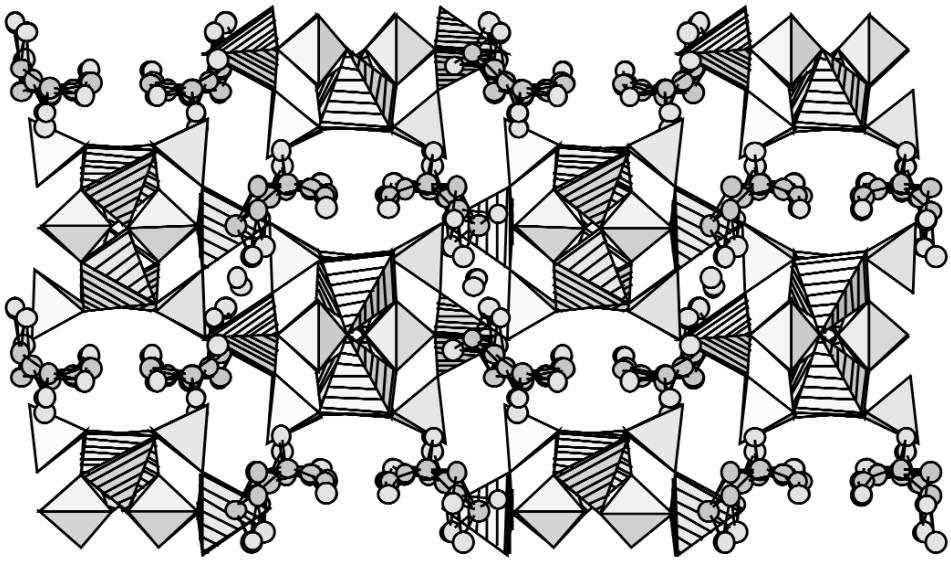

Fig. 4 The zinc phosphate layers intercalated with organic species; ZnO_4 tetrahedra are dashed, PO_4 tetrahedra are gray, C, N, and O atoms from organic molecules are gray circles.

The parallel inorganic layers are held together by being H-bonded to the intercalated species and adjacent layers. The three types of intercalated species (H_2DAP^{2+} ions, H_2mal, and NH_4^+ ions) are present with partial occupancies at similar positions in the structure. The partial occupancies were determined after the examination of bond and contact distances, which exclude simultaneous presence of some molecules. The NH_4^+ ion and one position of H_2DAP^{2+} ion are mutually present; in contrast, H_2mal and the other position of H_2DAP^{2+} ion can each be present only alone at a given site. Additionally, the position of NH_4^+ cation can only be up to 50 % occupied [the distance between N3 and symmetry-related N3 site is only 1.88(3) Å]. The refined structure with two positions of H_2DAP^{2+} ion (50 and 25 % occupied), one position of malonic acid (25 % occupied), and one position of amine cation (50 % occupied), was in agreement with elemental analysis (Fig. 5). The carbon–oxygen and carbon–nitrogen bond lengths are in general in agreement with the data found in a related system (Table 3) [35]. The deviations of some bond lengths from expected values are due to the described disorder. The intercalated species are connected together and with inorganic layers through H bonds with bond distances ranging from 2.19(6) to 3.06(1) Å (Table 4). The three short H-bond distances of 2.19(6), 2.24(6), and 2.29(8) Å are due to disorder of the H_2mal and the large displacement parameters of the atoms involved in these bonds. Also, there are strong H bonds between the inorganic layers. The shortest H-bond length between O(9) and O(7) in adjacent inorganic layers is 2.576(6) Å. In general, H-bonding appears to be a key factor in stabilizing the ZPAM structure.

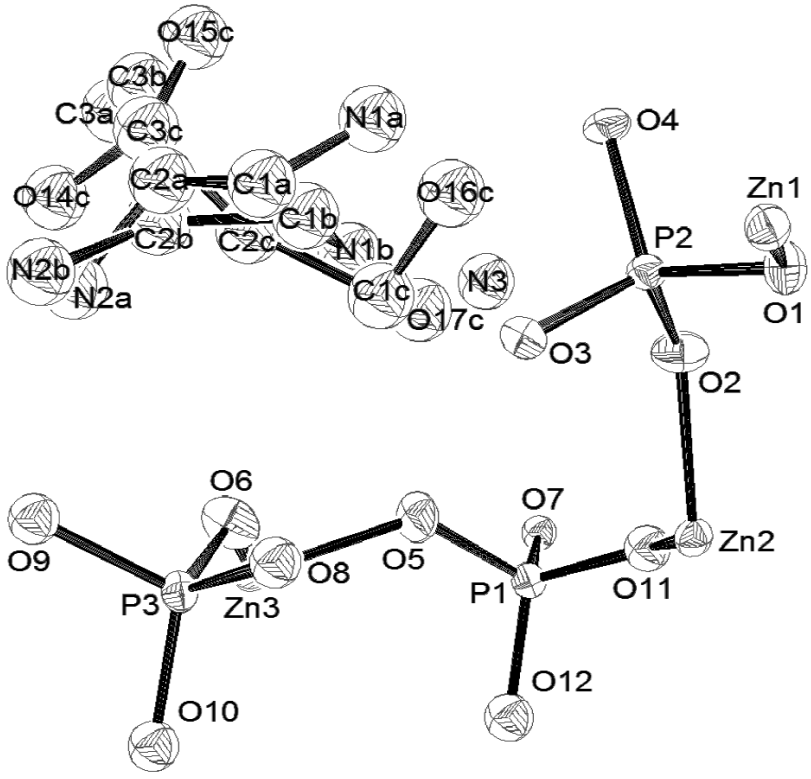

Fig. 5 Asymmetric unit of ZPAM structure with labeled atoms. Two positions of 1,2-diamine cation [atom labels with extension *a* (50 % occ.) or *b* (25 % occ.)] and malonate molecule [atom labels with extension *c* (25 % occ.)] are disordered as described in the text. N3 represents amine group (50 % occ.). All H atoms are omitted for clarity.

DISCUSSION

The use of malonic acid in the synthesis of open-framework structures has led to the formation of a new 2D zinc phosphate structure. The malonate ion has not shown the propensity to participate in the lattice formation and did not act as a ligand to the Zn atoms; instead, the malonic acid molecules in ZPAM remain intercalated between the layers. This behavior is in contrast to that of oxalic acid, since the oxalate ion has proved to be quite a suitable building block in the formation of hybrid networks [27–29,35]. This difference in behavior should be attributed to the structural differences between the two ions. Namely, the strict resonance-induced planarity of the free oxalate ion makes this anion in effect a rather rigid structural unit of fixed geometry, thus suitable to function as a building block of hybrid network systems. In contrast, the complete rotational freedom around two C–C axes in the malonate ion renders this anion a very flexible species that can be present in reaction systems in a variety of conformations. It is this lack of structural rigidity that seems to prevent the malonate ion from being an effective building block of network structures. In the same context, it is worth noticing that during the crystallization of ZPAM, the DAP species partially decomposed, yielding NH_4^+, so that in this system both the doubly protonated DAP and NH_4^+ ions exert a structure-directing role. This behavior is similar to that observed in the aluminophosphate synthesis in the presence of DAP, but in the absence of oxalate ions [36]. However, if oxalic acid is used in the latter synthesis, no decomposition of DAP is observed, and a 3D structure arises in which the (Al,O)- and (P,O)-polyhedra are cross-linked with oxalate ions [35]. It is likely that this cross-linking takes place around the DAP species at an early stage of crystallization, so that DAP is trapped and stabilized within the framework and does not undergo a

partial decomposition observed in the absence of oxalate ions. Since in the ZPAM synthesis the malonate ions do not cross-link with the (Zn,O)- and (P,O)-polyhedra, no such entrapment of the DAP species occurs and the latter does undergo a partial decomposition.

ACKNOWLEDGMENTS

We are thankful for the support by the Slovenian Ministry of Education, Science and Sport through the research program P0-0516-0104 and by the Ministry of Science and Technology of Serbia (Project No: OI 1603).

REFERENCES

1. W. T. A. Harrison and M. L. F. Phillips. *Chem. Commun*. 2771 (1996).
2. S. Neeraj, S. Natarajan, C. N. R. Rao. *New J. Chem.* 303 (1999).
3. Guo-Yu Yang and S. C. Slavi. *J. Am. Chem. Soc*. **121**, 8389 (1999).
4. J. N. Xu, Y. H. Yuan, Y. G. Mao, S. H. Shi, Y. K. Lee, T. S. Chang, T. Y. Song, S. H. Feng, R. R. Xu. *Chem. J. Chin. Univ.-Chinese* **21**, 509 (2000).
5. A. Choudhury, S. Natarajan, C. N. R. Rao. *Inorg. Chem.* **39**, 4295 (2000).
6. K. O. Kongshaug, H. Fjellvag, K. P. Lillerud. *Microporous Mesoporous Mater.* **39**, 341 (2000).
7. W. T. A. Harrison. *Acta Cryst., Sect. E* **57**, 248 (2000).
8. A. Simon, L. Josien, V. Gramlich, J. Patarin. *Microporous Mesoporous Mater*. **47**, 135 (2001).
9. H. Y. Ng and W. T. A. Harrison. *Microporous Mesoporous Mater.* **50**, 187 (2001).
10. S. Neeraj and S. Natarajan. *J. Phys. Chem. Solids* **62**, 1499 (2001).
11. L. A. Garcia-Serrano, F. Rey, J. Perez-Pariente, E. Sastre. *Thermochim. Acta* **376**, 155 (2001).
12. M. Wiebcke. *J. Mater. Chem*. **12**, 421 (2002).
13. Y. N. Zhao, X. M. Chen, X. H. Li, R. J. Wang, Z. H. Mai. *J. Solid. State Chem*. **165**, 182 (2002).
14. A. Simon-Masseron, J. L. Paillaud, J. Patarin. *Chem. Mater*. **15**, 1000 (2003).
15. P. Zhang, Y. Wang, G. S. Zhu, Z. Shi, Y. L. Liu, H. M. Yuan, W. Q. Pang. *J. Solid State Chem.* **154**, 368 (2000).
16. K. O. Kongshaug, H. Fjellvag, K. P. Lillerud. *Solid State Sci*. **2**, 569 (2000).
17. A. Choudhury, S. Natarajan, C. N. R. Rao. *J. Solid State Chem*. **157**, 110 (2001).
18. A. Echavarria and C. Saldarriaga. *Microporous Mesoporous Mater.* **42**, 59 (2001).
19. S. Natarajan. *J. Chem. Soc., Dalton Trans.* 2088 (2002).
20. M. Wiebcke. *J. Mater. Chem.* **12**, 143 (2002).
21. Y. Xing, Z. Shi, P. Zhang, Y. L. Fu, C. Cheng, W. Q. Pang. *J. Solid State Chem*. **163**, 364 (2002).
22. A. A. Ayi, S. Neeraj, A. Choudhury, S. Natarajan, C. N. R. Rao. *J. Phys. Chem. Solids* **62**, 1481 (2001).
23. S. Fleith, L. Josien, A. Simon-Masseron, V. Gramlich, J. Patarin. *Solid State Sci.* **4**, 135 (2002).
24. Z.-E. Lin, J. Zhang, S.-T. Zheng, G.-Y. Yang. *Inorg. Chem. Commun*. **6**, 1035 (2003).
25. S. Neeraj, S. Natarajan, C. N. R. Rao. *J. Solid State Chem*. **150**, 417 (2000).
26. C. N. R. Rao, S. Natarajan, A. Choudhury, S. Neeraj, R. Vaidhyanathan. *Acta Cryst.* **B57**, 1 (2001).
27. C. N. R. Rao. *Ind. J. Chem*. **42A**, 2163 (2003).
28. S. Neeraj, S. Natarajan, C. N. R. Rao. *J. Chem. Soc., Dalton Trans.* 289 (2001).
29. S. Natarajan. *Solid State Sci*. **4**, 1331 (2002).
30. C. Ruiz-Perez, Y. Rodriguez-Martin, M. Hernandez-Molina, F. S. Delgado, J. Pasan, J. Sanchiz, F. Lloret, M. Julve. *Polyhedron* **22**, 2111 (2003).
31. R. Vaidhyanathan, S. Natarayan, C. N. R. Rao. *J. Chem. Soc., Dalton Trans.* **8**, 1459 (2003).
32. A. Altomare, M. C. Burla, M. Camalli, G. Cascarano, C. Giacovazzo, A. Guagliardi, A. G. G. Maliterni, G. Polidori, R. Spagna. *J. Appl. Cryst*. **32**, 115 (1999).

33. G. Sheldrick. SHELXL-97, Gottingen (1997).
34. W. T. A. Harrison, J. A. Rodgers, M. L. F. Phillips, T. M. Nenoff. *Solid State Sci.* **4**, 969 (2002).
35. N. Rajic, N. Zabukovec Logar, G. Mali, V. Kaucic. *Chem. Mater*. **15**, 1734 (2003).
36. N. Rajic, N. Zabukovec Logar, A. Golobic, V. Kaucic. *J. Phys. Chem. Solids* **64**, 1097 (2003).